

Infiltration and Top Seed Growth-Textured YBCO Bulks With Multiple Holes

Jacques G. Noudem,^{†,‡} Sophie Meslin,[‡] Daniel Horvath,^{‡,§} Christelle Harnois,[‡] Daniel Chateigner,[‡] Bachir Ouladdiaf,[¶] Sophie Eve,[‡] Moustafa Gomina,[‡] Xavier Chaud,^{||} and Masato Murakami^{††}

[‡]CRISMAT, CNRS/UMR 6508, ENSICAEN and Université de Caen Basse-Normandie, 14050 CAEN, Cedex, France

[§]Supertech Laboratory, Department of Power Engineering, Budapest University of Technology and Economics, Budapest, Hungary

^{||}CRETA/CNRS, 38042 Grenoble, Cedex 09, France

^{††}Shibaura Institute of Technology, Tokyo 135-8548, Japan

[¶]Institut Laue-Langevin, BP 156-38042 Grenoble, Cedex 09, France

The recently reported hole-patterned $\text{YBa}_2\text{Cu}_3\text{O}_y$ (Y123) bulks with improved superconducting properties are highly interesting from material quality and application variety points of view. It is well known that the core of plain bulk superconductors needs to be fully oxygenated and some defects like cracks, pores, and voids must be suppressed in order that the material can trap a high magnetic field or carry a high current density. To minimize the above defects, we have used a combination of standard superconducting ceramic processing and an infiltration technique to prepare regularly perforated $\text{YBa}_2\text{Cu}_3\text{O}_y$ (Y123) bulk superconductors. This process leads to negligible shrinkage upon annealing and a uniform distribution of Y211 inclusions. Texture was evidenced by neutron pole figure measurements. Flux mapping was used to verify the superconducting homogeneity of the samples and to investigate the field-trapping ability. In addition, the textured drilled samples were reinforced using resin or metal impregnation and the influence of the different processing steps on the hardness of the materials has been investigated.

I. Introduction

It is well established that the critical current density J_c is closely related to the microstructural features in the melt-processed $\text{REBa}_2\text{Cu}_3\text{O}_y$ (RE = rare earth) samples.^{1–4} Dense materials with oriented single domains, free of cracks, voids, or porosity, are necessary to obtain large J_c . The conventional melt processing of $\text{REBa}_2\text{Cu}_3\text{O}_y$ involves shrinkage⁵ of the preform up to 25% due to the liquid-phase outflow, resulting in distortions and macrodefects. Like directed metal oxidation (DIMOX) or pressureless metal infiltration (PRIMEX),^{6,7} which have been commonly used as near-net shape ceramic-processing techniques, where the molten liquid alloy is allowed to infiltrate into the porous preform, several works^{8–14} have been reported for bulk $\text{REBa}_2\text{Cu}_3\text{O}_y$ using a similar infiltration-growth process. This technique is compatible with processing the material into near-net shapes free of porosity and at the same time yields highly textured material as a single domain. In addition, the papers dealing with these infiltration processes

mention the uniform distribution of fine grains of Y211, Sm211, or $\text{Nd}_4\text{Ba}_2\text{Cu}_2\text{O}_y$ (Nd422) inclusions (insulating phase) in the superconducting $\text{REBa}_2\text{Cu}_3\text{O}_y$ matrix (where RE = Y, Sm, or Nd). It is also well known that during the oxygen annealing-inducing superconductivity, cracks open at the surface layer and propagate into the bulk.^{15,16} To overcome such problems, the perforated geometry offers a significant potential in helping the oxygenation process, avoiding crack developments, and increasing mechanical reinforcement.

In this study, we have used the infiltration and top seed growth (ITSG) processes to prepare textured Y123/Y211 composites. Additionally, textured bulks of YBCO with multiple holes were processed and characterized using neutron-preferred orientation measurements and magnetic flux mapping, and the mechanical properties of the different samples have been compared.

II. Experimental Procedure

The details of ITSG and multiple holes process of $\text{YBa}_2\text{Cu}_3\text{O}_y$ (Y123) are reported elsewhere.¹³ Basically, The $\text{Y}_2\text{Ba}_1\text{Cu}_1\text{O}_y$ (Y211) block or pellet was placed on top of the liquid phase ($3\text{BaCuO}_2 + 2\text{CuO}$) or $\text{Ba}_3\text{Cu}_5\text{O}_8$ (Y035) to allow the liquid infiltration driving by capillarity force. An Sm123 seed as a nucleation center was placed on the top of the Y211 preform. The holes in the preform were realized by drilling cylindrical cavities with a diameter of 0.5–2 mm through the circular or square-shaped sample. The holes are arranged in a regular network in the plane of the samples (Fig. 1).

DC magnetization measurements were performed on square-shaped samples, selected from the single domains, using a SQUID magnetometer (Quantum Design, Oxford, U.K.) to determine the critical transition temperature, T_c , and critical current density, J_c , under a magnetic field. J_c was estimated using the extended Bean critical state model. Normal electrical contacts between the samples and current leads were prepared by painting commercial silver paste (Dupont 4929, Bristol, U.K.). The samples were annealed in flowing oxygen at 900°C for half an hour to ensure a good silver diffusion, followed by oxygenation at 450°C for 150 h. The typical contact resistances were $< 1 \mu\Omega \cdot \text{cm}^2$ at 77 K. The transport critical current measurements, J_c^t , were performed using a 600 A power supply (MB-Electronique Inc., Buc, France) at 77 K in self-field. In addition, the magnetization hysteresis loops of all samples were measured at 77 K using a SQUID magnetometer.

The capability of the whole sample to carry supercurrents in large current loops in the sample volume has been investigated

P. Paranthaman—contributing editor

Manuscript No. 22656. Received January 22, 2007; approved May 2, 2007.

The authors wish to acknowledge the financial support from Conseil Régional de Basse Normandie, France.

[†]Author to whom correspondence should be addressed. e-mail: jacques.noudem@ensicaen.fr

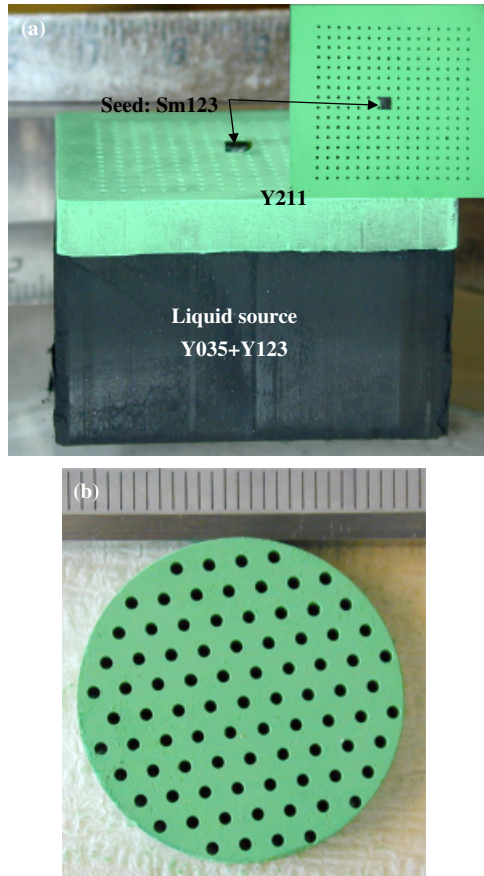


Fig. 1. (a) Configuration (cross section) used for converting the mechanically drilled Y_2BaCuO_5 into a single grain of $\text{YBa}_2\text{Cu}_3\text{O}_{7-\delta}$ by the infiltration and growth process. The Sm123 seed crystal used for nucleation is placed on the surface of the perforated structure. The inset shows the top view with artificially patterned holes ($\Phi = 0.5$ mm). (b) Top view of the multiple hole ($\Phi = 1$ mm) Y211 pellet.

using magnetic flux trapping. In such measurements, the sample is first cooled down to 77 K in a 2 T magnetic field delivered by a superconducting coil. In a second step, the magnetic field is removed and the sample surface is scanned with a Hall probe at 1 mm of the surface using a 0.5 mm grid step.

In order to estimate the influence of the holes and the impregnation phases on the mechanical properties of the samples, we have determined the Vickers hardness of hole-free specimens, of nonimpregnated-drilled samples (hole diameters of 0.5 and 1

mm), and drilled samples impregnated by metal (hole diameters of 0.5 and 1 mm) and resin (holes diameter of 0.5 mm).

The Vickers indentations were operated on polished surfaces by means of a Zwick testing machine. Before the test, a thin gold layer (500 Å) was sputtered on the polished surfaces of the samples, in order to obtain a clean-looking impression. A 14.7 N load was applied for 15 s and the hardness was determined from the usual relationship

$$H_v = \frac{1.854P}{4a^2}$$

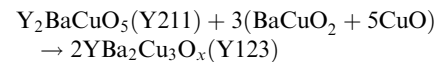
where a is the mean half-diagonal of the square-shaped hardness imprint (see Fig. 9(a)).

For the drilled specimens (impregnated or not), the influence of the stress states around the holes on the hardness was investigated by performing tests in the “bulk” of the drilled samples, between two holes (+ in Fig. 9(b)) and between four holes (\times in Fig. 9(b)). “Bulk” refers to central positions “far away” from the holes, but also not too close to the center, as the values could be influenced by the seed.

III. Results and Discussion

(1) Infiltration-Growth Single Domains

A typical as-grown bulk sample obtained from the ITSG-process is shown in Fig. 2. The trace of the faceted growth on the surface reveals that a single-domain pellet has been successfully elaborated. The vertical shine trace on the side of the pellet demonstrates that the domain has grown on the whole thickness of the pellet. One can clearly observe the strong shrinkage of the liquid source with respect to the Y211 preform, which has been converted to Y123 during the process following the chemical reaction:



We could also observe that after the process, the Y123 pellet (Fig. 2) nearly maintained its original dimensions with a maximum shrinkage of around 10%. This value is about half the one observed for the conventional melt-textured samples.⁵ Optical micrographs of polished surfaces (Fig. 3) of the samples reveal the typical microstructural features known¹³ from melt-processed bulk materials. In the present ITSG process, no specific efforts like doping^{17,18} or irradiation¹⁹ have been made to optimize the Y211 particle size and defect density in further

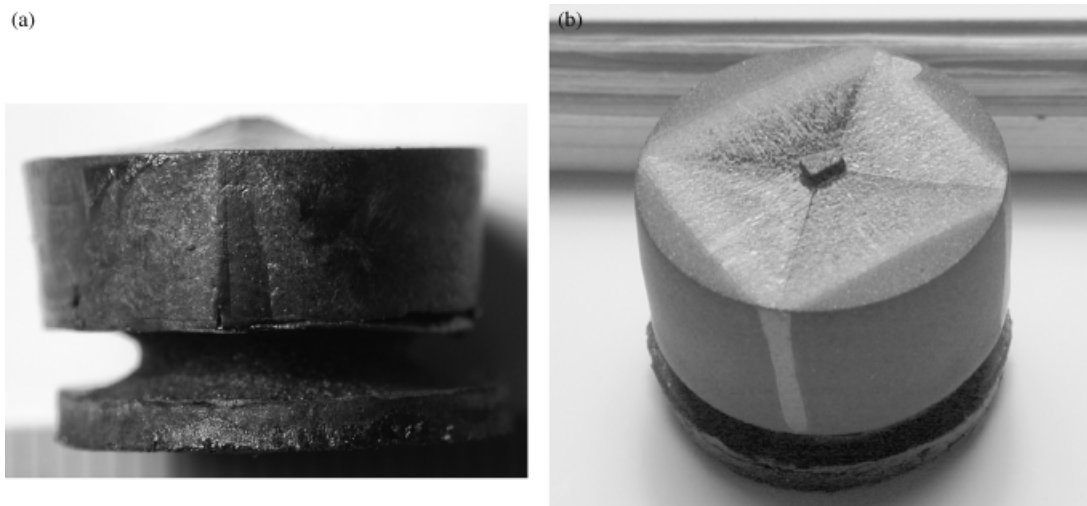


Fig. 2. An as-grown bulk sample obtained by infiltration and top seed growth showing the strong shrinkage of the source (a) and the single-grain growth along the whole height of the pellet, as evidenced by the contrast on the top view (b).

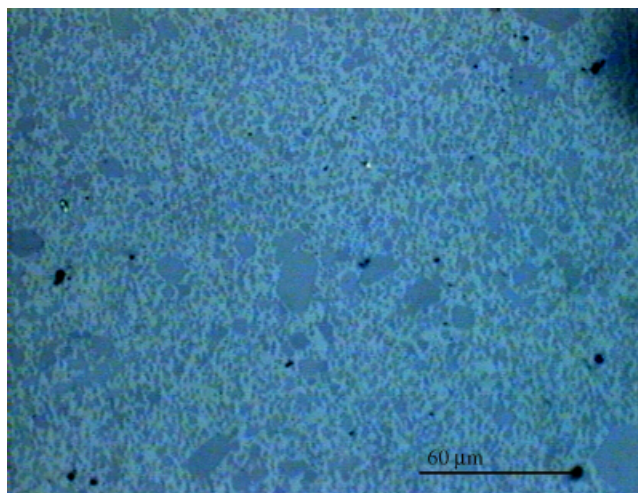


Fig. 3. Microstructures of the samples prepared by infiltration and top seed growth.

improving the critical current densities. The average size of Y211 particles is determined at 1 μm for the ITSG samples compared with 2.4 μm for conventional TSMTG¹³ ones. Moreover, a uniform distribution of Y211 inclusions could be seen in the ITSG microstructure. The small size of Y211 particles obtained without any doping is clearly one advantage of the combination of infiltration and top seeding growth. This refinement of Y211 inclusions is very probably the reason for good flux pinning and high critical current densities in our ITSG samples. The homogeneous distribution of Y211 inclusions in the ITSG samples can be explained by the small Y211 particles used in the Y211 preform, which are further dissolved in the liquid phase to form a Y123 phase resulting in finer spherical Y211 particles in contrast to the larger acicular size Y211 and their inhomogeneous distribution in the sample processed conventionally without any dopants.¹³

The temperature dependence of the magnetization showed a sharp transition width of 1 K with $T_c \sim 91$ K, for all samples. The magnetic field was applied parallel to the pellet axis. The magnetic, J_c values are estimated for this direction from M to H cycles by applying the extended Bean critical-state relation,²⁰ as derived from

$$J_c = 20\Delta M/[a(1 - (a/3b))]$$

where ΔM is the magnetic hysteresis measured in emu/cm^3 , and a and b are the sample dimensions (with $a < b$) in cm. At 77 K and self-field, the J_c values are 86 000 A/cm^2 for the ITSG sample, compared with 10 000 and 90 000 A/cm^2 for the TSMTG, without and with dopants, respectively. These values are comparable with those reported in the literature.^{21–23} We can also

note that Delamare *et al.*¹⁷ and Iida *et al.*²³ reported J_c values of 5.5×10^4 and 6×10^4 A/cm^2 , respectively, obtained on melt-textured YBCO.

The addition of Pt or CeO_2 is believed to reduce the interfacial energy between Y211 and the liquid phase, and to consequently reduce the growth of Y211 particles. The refinement of Y211 using Pt addition leads to beneficial flux pinning and a high-critical current density. Noticeably, in ITSG samples, high J_c 's are obtained without doping, while such a doping is necessary in TSMTG samples. For ITSG samples, DC transport J_c^t 's of 4.3×10^4 A/cm^2 at 77 K in the self-field have been measured, demonstrating their ability to carry high-critical transport current density.

(2) Perforated Samples

Cubic- or cylindrically shaped pellets of the Y211 preform were used to grow single domains of Y123 by TSMTG and ITSG processes using the configuration described in Fig. 1. The usual growth lines at the surface of the domains have been obtained. This has been confirmed using video imaging²⁴ of the melt-growth process, and on other perforated samples,^{25–27} strongly indicating that the presence of the holes does not disturb the growth as a single domain in the volume. Figure 4 shows cross sections of plain (right) and perforated (left) ITSG samples. As major information, porosity is strongly reduced in the drilled sample, whereas the plain sample exhibits large porosities and cracked zones. A SEM observation between two holes clearly illustrates (i) a compact, crack-free microstructure and (ii) uniform distribution of the fine Y211 particles into the Y123 matrix.

(3) Trapped Field Distribution

The trapped magnetic flux mappings of the plain and drilled samples (36 mm diameter and 15 mm height) are presented in Figs. 5(a) and (b), respectively. The samples, conventionally oxygenated at 450°C for 150 h, were previously magnetized at 2 T, 77 K, using a superconducting coil. The 3D representation of the trapped magnetic flux roughly shows a single dome in both cases, corresponding to the signature of a single domain. We can then conclude that the network of holes did not significantly affect the current loops at the macroscopic scale, except for the empty volumes created in the material. This result is supported by the neutron quantitative texture analysis showing only one single domain with mean c -axis at only around 10° from the pellet axis in the whole volume for the perforated ITSG sample (Fig. 6(a)), with the {003} pole figure showing a maximum of density around 95 m.r.d. (95 time the random value). Interestingly, the {003} pole figure of the plain sample (Fig. 6(b)) exhibits a more distributed pole of a somewhat lower maximum density at 42 m.r.d., and small volume contributions corresponding to c -axis at 90° from the pellet axis (poles located on the equator of Fig. 6(b)). This observation could signify that the better oxygenation of the structure due to the increased surface

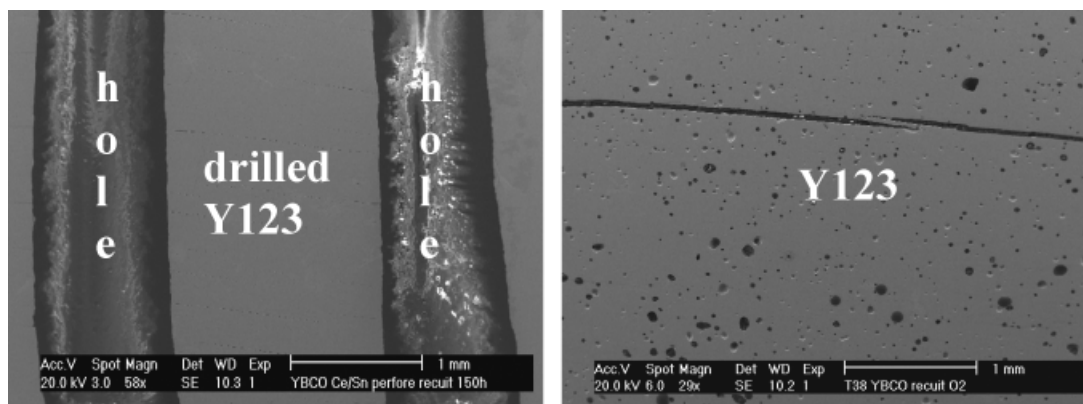


Fig. 4. Resulting microstructures of the drilled (left) and plain (right) samples.

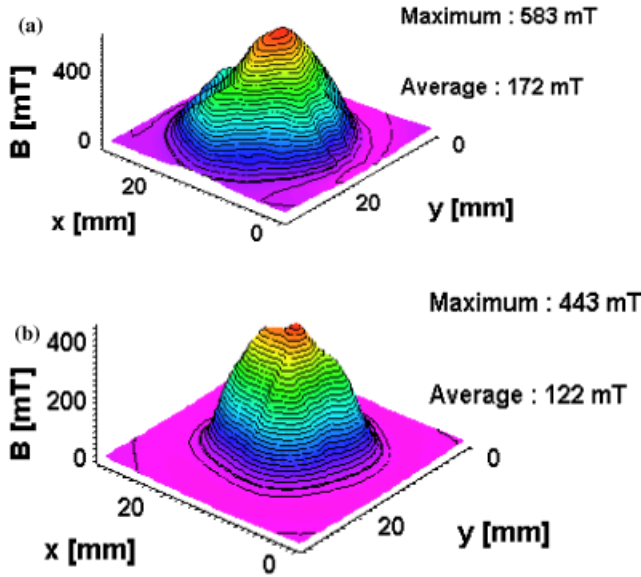


Fig. 5. Trapped magnetic flux measurements on (a) drilled and (b) plain samples.

exchange provided by the holes also enhances the texture, at least for crystals whose orientation is close to the main component (main central pole of the {003} pole figure), or for crystals in a twinned relationship with the main component (poles on the equator). Such a behavior could be obtained by partial recrystallization and/or oxygen diffusion during the oxygenation process. Correlatively, the trapped field value is larger in the perforated (583 mT) than in the plain (443 mT) sample. This represents an increase of 32% for the drilled sample, in agreement with our previous report²⁵ and with the neutron texture analysis. This increase in the trapped field is possibly due to: (i) a better oxygenation and/or less cracks and porosities for the drilled pellet as illustrated in Fig. 4(b) and an increase in surface exchange, (ii) a stronger pinning due to the larger hole/solid phase area, or (iii) a cooling enhancement by a more intimate

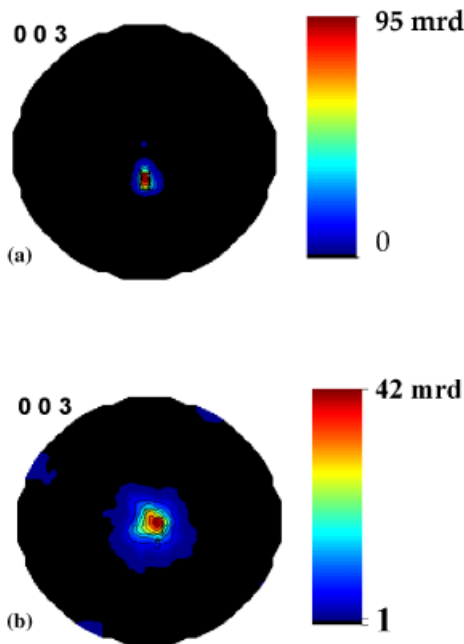


Fig. 6. Neutron {003} pole figures recalculated from the ODF (a) drilled and (b) plain samples. Logarithmic density scale, equal area projection.

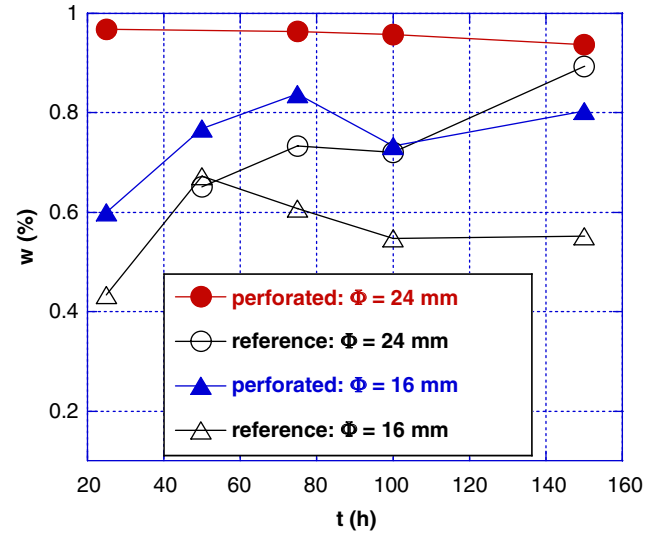


Fig. 7. Influence of oxygen annealing showing the oxygen uptake into the drilled and plain samples for 16 and 24 mm diameter cylinders.

contact with liquid nitrogen. This last point can be useful during application to avoid hot spots at high currents, e.g. in fault current limiters (FCL).

(4) Effect of Oxygenation Duration

According to their thin-wall geometry, the drilled samples should be more oxygenated than the plain samples, because after an easy diffusion through the tube channels, oxygen can diffuse in volumes, which could not be reached during the annealing time without holes. Thermogravimetry has been chosen to compare the oxygen uptake of our samples with and without holes. In this study, 16- and 24-mm-diameter pellets have been used and a network of 30 holes have been drilled. For each diameter, five drilled and five plain samples have been measured

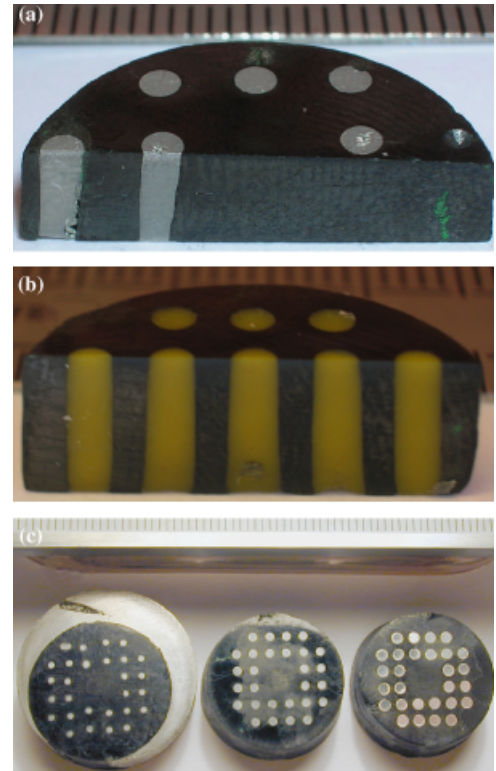


Fig. 8. Reinforcement of the drilled samples by impregnation with (a) an Sn/In alloy, (b) with wax resin and (c) top views of the samples filled with a BiPbSnCd alloy.

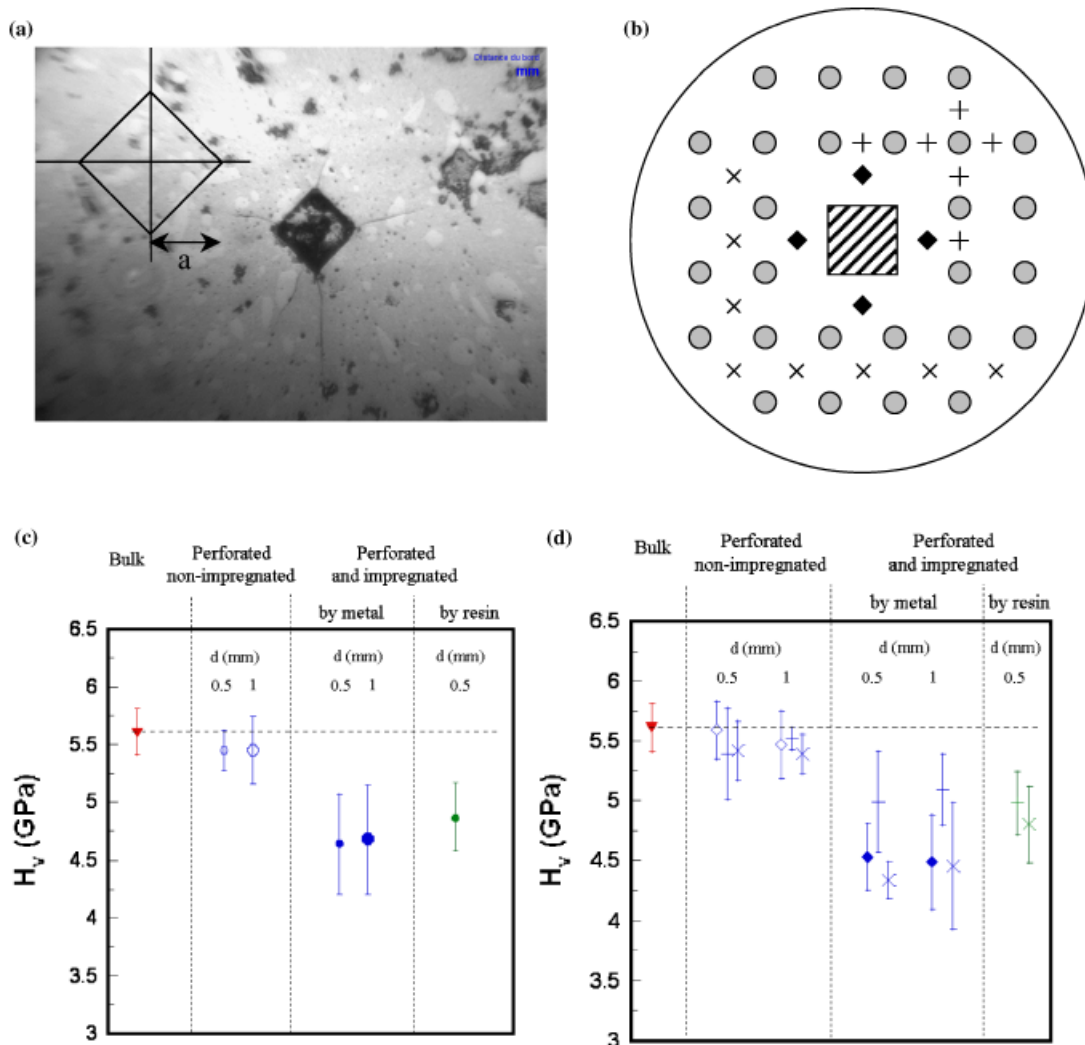


Fig. 9. (a) Optical micrograph showing a Vickers indentation in a hole-free and impregnation-free sample; (inset) sketch of the Vickers indentation. (b) Sketch of the different indentation positions on the drilled specimens (◆, in the “bulk”; +, between two holes; ×, between four holes) (the seed imprint shows the dashed square in the middle of the sample). (c) Hardness values determined on the different samples; (d) influence of the indentation location on the hardness values (◆, in the “bulk”; +, between two holes; ×, between four holes).

by thermogravimetry under the same thermal conditions. From the initial (w_i) and final (w_f) weights, the relative weight gain in oxygen is estimated

$$w(\%) = 100(w_f - w_i)/w_i$$

The measurements have been operated twice to check for reproducibility, samples being de-oxygenated at 900°C, half an hour, and then quenched, between the two measurements. After the second measurement, the average weight values were calculated (Fig. 7). Clearly, the oxygenation of the perforated samples is fully operated after only 25 h, whereas plain samples need more than 150 h under the same annealing conditions (400–450°C under flowing O₂).^{15, 25, 27, 28}

(5) Reinforcement of the Drilled Samples

The Y123 domain with open holes could be reinforced, e.g. by infiltration with a low-melting metal alloy, to improve the mechanical properties useful for levitation applications and trapped field magnets. The perforated Y123 bulk with 1- or 2-mm-diameter holes were dipped into a molten Sn/In alloy or epoxy wax at 70°C for 30 min in a pressure vessel after evacuating the chamber with a rotary pump and venting in air to enable the molten alloy or liquid resin to fill up the holes. After cooling, the impregnated bulk materials were polished. Some samples have been impregnated with a BiPbSnCd alloy using a

process described elsewhere.²⁹ Figure 8 shows the top surface and a cross-sectional view of the impregnated Y123 bulk samples. We can notice the dense and homogeneous infiltration of the wax epoxy and Sn/In alloy. The magnetic flux mapping of the sample filled with a BiPbSnCd alloy has been investigated. The same maximum trapped field of 250 mT before and after impregnation has been measured. Presently, it is important to develop specific shapes of bulk superconductor with improved mechanical properties for any practical application. Different papers have already reported and demonstrated the reinforcement of bulk superconductor materials. Krabbes and colleagues,^{30,31} for example, observed that reinforcing Y123 monoliths with steel bandages and banding with high-strength steel rings enables large grain samples to trap magnetic fields of 16 T at 24 K. In addition, Tomita and Murakami³² reported trapped fields of 17 T at 29 K for a YBCO monolith after resin impregnation and wrapping the sample in carbon fiber.

(6) Hardness

The measured Vickers hardness of the bulk sample (i.e. non-impregnated hole-free material) is about 5.6 GPa, which is in good agreement with different values reported in the literature.^{33,34} Figure 9(c) shows the average values (average of eight measures on the nonperforated samples, 18 measures on the other samples) of the hardness for the different studied samples. The large scatter of the experimental values is explained by the coarse microstructure of the materials and the local investigation

technique used. Comparison of the hardness values of the bulk with those obtained from nonimpregnated drilled samples indicates that the presence of the holes has no significant influence on the hardness of the material, whatever the diameter of the holes, in the investigated size range. The impregnation of the drilled samples, by metal alloy or resin, results in a decrease of the hardness of the samples. This softening was expected as a consequence of the introduction of a smoother phase into the superconductor material. Moreover, as the resin is harder than the metal alloy, the hardness value of the resin-impregnated sample was expected to be higher than the metal-impregnated ones, but this trend has not been clearly verified. Figure 9(d) presents the hardness values as a function of the different locations in the samples. According to these results, no clear trend can be established between the hardness and the location of the test point, except for the metal-impregnated samples for which the hardness is somewhat higher between two holes than in the bulk or between for holes.

(7) Outlook

Porous ceramic materials, such as alumina and zirconia, are established components in a number of industrial applications such as inkjet printer, fuel injection systems, filters, structures for catalysts, elements for thermal insulation, and flame barriers. The combination of a high specific surface with the ability to be reinforced in order to improve mechanical and thermal properties makes the perforated YBCO superconductors interesting candidates both for a variety of novel applications and for fundamental studies. As an example, the artificially drilled Y123 into a desired structure^{35,36} is a good candidate for resistive elements in superconducting FCL.^{37,38} In this application, the thin wall between the holes allows more efficient heat transfer between a perforated superconductor and a cryogenic coolant during an overcurrent fault compared with conventional bulk material. The high surface area of the perforated materials, which may be adjusted by varying the hole diameter, makes them interesting candidates for studying fundamental aspects of flux pinning, because the extent of surface pinning, and hence J_c , are expected to differ significantly from bulk YBCO grains of similar microstructure. This new structure has great potential for many applications with improved performances in place of Y123 hole-free bulks, because it should be easier to oxygenate, and to maintain at liquid nitrogen temperature during application, avoiding the hot-spot occurrence. For meandering FCL elements, cutting is a crucial step as cracks appear during this stage. This can be solved by *in situ* zigzag shape processing of holes as we demonstrated the feasibility elsewhere.³⁵ The study of the mechanical properties of the different samples may be extended by determining the toughness of the materials, i.e. their resistance to crack propagation, from the indentation cracks.

IV. Conclusion

Single-grain Y123 superconductors have been grown by liquid infiltrating from a Y035 source into a Y211 preform. The infiltration-growth method allows processing of a Y123 single domain, with a homogeneous distribution of Y211 into the Y123 matrix. The critical current density at 77 K and the self-field was determined to be 86 000 A/cm², which is close to the best values measured on samples prepared by the conventional TSMTG process. The present ITSG process is simple and has both technical and cost advantages compared with the existing TSMTG technique.

In addition, the textured Y123 bulks with multiple holes have been processed and characterized. SEM studies have shown that the holes' presence does not hinder the domain growth. The perforated samples exhibit a *c*-axis grain orientation confirmed by pole figure and the single-domain character is evidenced by trapped-field distribution. This new structure has great potential for many applications with improved performances in place of Y123 hole-free bulks because it should be easier to maintain at

liquid nitrogen temperature during application, avoiding the appearance of hot spots. It is clear that the Y123 bulks with an artificial pattern of holes are beneficial to evacuate porosity from the bulk and to uptake the oxygen.

The ability of the Y123 with multiple holes to trap a high field has been demonstrated. At 77 K, the trapped field value for the drilled samples is 32% larger than in the plain ones. Superconducting bulks with an artificial array of holes can be filled with metal alloys or high-strength resins to improve their thermal properties, without any significant decrease in the hardness, to overcome the built-in stresses in levitation and quasi-permanent magnet applications. Further investigations concerning other mechanical properties of practical interest, the influence of hole density, and interconnected arrays of holes on the transport properties are under way.

Acknowledgments

The authors would like to thank the EFFORT consortium (European Forum for Processors of Large Grain (RE)BCO Materials (<http://www.rebco-effort.net>) for providing an encouraging environment to pursue the development of single-domain (RE)BCO bulk samples. Meslin and D. Horvath are grateful the French "Ministère de la Recherche et de la Technologie" for PhD financial support.

References

- ¹M. Murakami, "Melt-Processing of High Temperature Superconductors," *Prog. Mater. Sci.*, **38**, 311–57 (1994).
- ²K. Salama and S. Sathyamurthy, "Melt Texturing of YBCO for High Current Application," *Appl. Supercond.*, **4** [10–11] 547–61 (1996).
- ³M. Morita, M. Tanaka, S. Takebayashi, K. Kimura, K. Miyamoto, and K. Sawano, "Effect of Pt Addition on Melt-Processed YBaCuO Superconductors," *Jpn. J. Appl. Phys.*, **30**, L813–5 (1991).
- ⁴S. Marinel, J. Wang, I. Monot, M. P. Delamare, J. Provost, and G. Desgardin, "Top-Seeding Melt Texture Growth of Single-Domain Superconducting YBa₂Cu₃O₇-Pellets," *Supercond. Sci. Technol.*, **10**, 147–55 (1997).
- ⁵E. S. Reddy and T. Rajasekharan, "Microstructural Studies of PrBa₂Cu₃O₇ During Melt Processing," *J. Mater. Res.*, **13**, 3389–92 (1998).
- ⁶A. W. Urquhart, "Novel Reinforced Ceramics and Metals: A Review of Lanthanide's Composite Technologies," *Mater. Sci. Eng. A*, **144**, 75–82 (1991).
- ⁷A. S. Nagelberg, "Observations on the Role of Mg and Si in the Directed Oxidation of Al–Mg–Si Alloys," *J. Mater. Res.*, **7**, 265–8 (1992).
- ⁸Y. L. Chen, H. M. Chan, M. P. Harmer, V. R. Todt, S. Sengupta, and D. Shi, "A New Method for Net-Shape Forming of Large, Single-Domain YBa₂Cu₃O_{6+x}," *Physica C*, **234**, 232–6 (1994).
- ⁹E. Sudhakar Reddy and T. Rajasekharan, "Fabrication of Textured REBa₂Cu₃O₇/RE₂BaCuO₅ (RE = Y, Gd) Composites by Infiltration and Growth of RE₂BaCuO₅ Preforms by Liquid Phases," *Supercond. Sci. Technol.*, **11**, 523–34 (1998).
- ¹⁰N. V. N. Viswanath, T. Rajasekharan, N. Harish Kumar, L. Menon, and S. K. Malik, "Infiltration–Growth Processing of SmBa₂Cu₃O₇ Superconductor," *Supercond. Sci. Technol.*, **11**, 420–5 (1998).
- ¹¹C.-J. Kim, Y. A. Jee, K.-W. Lee, T.-H. Sung, S.-C. Han, I.-H. Kuk, and G.-W. Hong, "Low Temperature Melt Process of SmBa₂Cu₃O_{7-y} using a Liquid Infiltration Technique," *Appl. Supercond.*, **6**, 149–56 (1998).
- ¹²N. Hari Babu, M. Kambara, P. J. Smith, D. A. Cardwell, and Y. Shi, "Fabrication of Large Single-Grain Y–Ba–Cu–O Through Infiltration and Seeded Growth Processing," *J. Mater. Res.*, **15**, 1235–8 (2000).
- ¹³S. Meslin and J. G. Noudem, "Infiltration and Top Seeded Grown Monodomain YBa₂Cu₃O_{7-x} Bulk Superconductor," *Supercond. Sci. Technol.*, **17**, 1324–8 (2004).
- ¹⁴H. Fang and K. Ravi-Chandar, "Fabrication of Y123 Disk by the Seeded Infiltration and Growth Method," *Physica C*, **340**, 261–8 (2000).
- ¹⁵D. Isfort, X. Chaud, R. Tournier, and G. Kapelski, "Cracking and Oxygenation of YBaCuO Bulk Superconductors: Application to C-Axis Elements for Current Limitation," *Physica C*, **390**, 341–55 (2003).
- ¹⁶P. Diko, G. Fuchs, and G. Krabbes, "Influence of Silver Addition on Cracking in Melt-Grown YBCO," *Physica C*, **363**, 60–6 (2001).
- ¹⁷M. P. Delamare, I. Monot, J. Wang, K. A. Provost, and G. Desgardin, "Influence of CeO₂, BaCeO₃ or PtO₂ Additions on the Microstructure and the Critical Current Density of Melt Processed YBCO Samples," *Supercond. Sci. Technol.*, **9**, 534 (1996).
- ¹⁸H. Walter, M. P. Delamare, B. Bringmann, A. Leenders, and H. C. Freyhardt, "Melt-Textured YBaCuO With High Trapped Fields Up To 1.3 T at 77 K," *J. Mater. Res.*, **15**, 1231–4 (2000).
- ¹⁹A. Wisniewski, R. M. Schalk, H. W. Weber, M. Reissner, and W. Steiner, "Comparison of Neutron Irradiation Effects in the 90 K and 60 K Phases of YBCO Ceramics," *Physica C*, **197**, 365–70 (1992).
- ²⁰E. M. Gyorgy, R. B. Van Dover, K. A. Jackson, L. F. Schneemeyer, and J. V. Waszczak, "Anisotropic Critical Currents in Ba₂YCu₃O₇ Analyzed Using an Extended Bean Model," *Appl. Phys. Lett.*, **55**, 283–5 (1989).
- ²¹K. Iida, N. H. Babu, Y.-H. Shi, and D. A. Cardwell, "The Effect of the Addition of Zirconium-Containing Compounds on the Microstructure and

Superconducting Properties of Mono-Domain Y–Ba–Cu–O Bulk Superconductors,” *Supercond. Sci. Technol.*, **18**, 704–9 (2005).

²²D. A. Cardwell, N. Hari Babu, Y. Shi, and K. Iida, “A Practical Processing Method for the Fabrication of High Performance, Single Grain (LRE)-Ba–Cu–O Superconductors,” *Supercond. Sci. Technol.*, **19**, S510–6 (2006).

²³K. Iida, N. Hari Babu, Y. Shi, and D. A. Cardwell, “Seeded Infiltration and Growth of Large, Single Domain Y–Ba–Cu–O Bulk Superconductors With very High Critical Current Densities,” *Supercond. Sci. Technol.*, **18**, 1421–7 (2005).

²⁴Video at webpage: www-crismat.ensicaen.fr/crismat/crismat.html

²⁵X. Chaud, S. Meslin, J.-G. Noudem, C. Harnois, L. Porcar, D. Chateigner, and R. Tournier, “Isothermal Growth of Large YBaCuO Single Domains Through an Artificial Array of Holes,” *J. Cryst. Growth.*, **275**, 855–60 (2005).

²⁶E. Sudhakar Reddy, N. Hari Babu, Y. Shi, D. A. Cardwell, and G. J. Schmitz, “Processing of Large Grain Y-123 Superconductors With Pre-Defined Porous Structures,” *Supercond. Sci. Technol.*, **18**, S15–8 (2005).

²⁷P. Diko, S. Kracunovska, L. Ceniga, J. Bierlich, M. Zeiberger, and W. Gawalek, “Microstructure of Top Seeded Melt-Grown YBCO Bulks With Holes,” *Supercond. Sci. Technol.*, **18**, 1400–4 (2005).

²⁸C. Leblond, I. Monot, D. Bourgault, and G. Desgardin, “Effect of the Oxygenation Time and of the Sample Thickness on the Levitation Force of Top Seeding Melt-Processed YBCO,” *Supercond. Sci. Technol.*, **12**, 405–10 (1999).

²⁹S. Nariki, N. Sakai, and M. Murakami, “Melt-Processed Gd–Ba–Cu–O Superconductor with Trapped Field of 3 T at 77 K,” *Supercond. Sci. Technol.*, **18**, S126–30 (2005).

³⁰G. Fuchs, S. Gruss, P. Verges, G. Krabbes, K.-H. Müller, J. Fink, and L. Schultz, “High Trapped Fields in Bulk YBCO Encapsulated in Steel Tubes,” *Physica C*, **372**, 1131–3 (2002).

³¹S. Gruss, G. Fuchs, G. Krabbes, P. Verges, G. Stover, K.-H. Müller, J. Fink, and L. Schultz, “Superconducting Bulk Magnets: Very High Trapped Fields and Cracking,” *Appl. Phys. Lett.*, **79**, 3131–3 (2001).

³²M. Tomita and M. Murakami, “High-Temperature Superconductor Bulk Magnets that can Trap Magnetic Fields of over 17 Teslas at 29 K,” *Nature*, **421**, 517–20 (2003).

³³F. Tancret, G. Desgardin, and F. Osterstock, “Influence of Porosity on the Mechanical Properties of Cold Isostatically Pressed and Sintered YBa₂Cu₃O_{7-x} Superconductors,” *Phil. Mag.*, **75**, 505–23 (1997).

³⁴M. Tomita, M. Murakami, K. Itoh, and H. Wada, “Mechanical Properties and Field Trapping Ability of Bulk Superconductors With Resin Impregnation,” *Supercond. Sci. Technol.*, **17**, 78–82 (2004).

³⁵J. G. Noudem, S. Meslin, C. Harnois, D. Chateigner, and X. Chaud, “Melt Textured YBa₂Cu₃O_y Bulks With Artificially Patterned Holes: A New Way of Processing c-axis Fault Current Limiter Meanders,” *Supercond. Sci. Technol.*, **17**, 931–6 (2004).

³⁶C. Harnois, S. Meslin, J.-G. Noudem, D. Chateigner, B. Ouladdiaf, and X. Chaud, “Shaping of Melt Textured Samples for Fault Current Limiters,” *IEEE Trans. Appl. Supercond.*, **15**, 3094–7 (2005).

³⁷R. Tournier, E. Beaugnon, O. Belmont, X. Chaud, D. Bourgault, D. Isfort, L. Porcar, and P. Tixador, “Processing of Large Y₁Ba₂Cu₃O_{7-x} Single Domains for Current-Limiting Applications,” *Supercond. Sci. Technol.*, **13**, 886–95 (2000).

³⁸P. Tixador, X. Obradors, R. Tournier, T. Puig, D. Bourgault, X. Granados, J. M. Duval, E. Mendoza, X. Chaud, E. Varesi, E. Beaugnon, and D. Isfort, “Quench in Bulk HTS Materials—Application to the Fault Current Limiter,” *Supercond. Sci. Technol.*, **13**, 493–7 (2000). □